CrystEngComm

COMMUNICATION

View Article Online
View Journal | View Issue

Cite this: *CrystEngComm*, 2024, **26**, 2131

Received 28th March 2024,
Accepted 28th March 2024

DOI: 10.1039/d4ce00307a

rsc.li/crystengcomm

Shortening C≡N···Br–C_{sp^3} halogen bonds *via* π-stacking†

Kamil Kupietz, [a] Rosa M. Gomila, [b] Thierry Roisnel, [a] Antonio Frontera *[b] and Rafael Gramage-Doria *[a]

The X-ray structure of 2-(dibromomethyl)benzonitrile, featuring unexpectedly short C≡N···Br halogen bond distances between a nitrile group and a C(sp^3)-linked bromine atom, is presented. Despite the weak Lewis base nature of the nitrile N atom and absence of strong electron-withdrawing groups on the Br atom, π-stacking significantly enhances both the electron donor and acceptor capability of the interacting partners. As such, and beyond trivial (hetero)aromatic systems, the rationale of C≡N···Br halogen bonding can also be employed in purely aliphatic systems.

Halogen bonding is increasingly recognized for its significance in various fields, including materials science,[1] catalysis,[2,3] and medicinal chemistry.[4,5] This interaction typically involves a heavy halogen atom, such as bromine or iodine, acting as an electrophile to form a highly directional noncovalent bond with a nucleophilic counterpart.[6] Typically, this nucleophile is an atom like nitrogen, oxygen, or sulfur, possessing a lone pair of electrons.[6,7] Halogens are amenable for participating in such interactions due to their unique electronic characteristics, which notably include a region of positive potential, termed the σ-hole, situated along the extension of their covalent bond.[8–10] In the realm of supramolecular chemistry and crystal engineering, halogen bonding stands out as a potent tool for designing and synthesizing novel materials.[11] Its appeal lies in the predictability, directionality, and tunability of these interactions, facilitating the precise organization of molecular components within crystal lattices. This precision is crucial for generating materials with unique properties and targeted functionalities.[12,13] The application of halogen bonding in crystal engineering not only enhances our comprehension of molecular interactions but also paves the way for novel methods in the design and development of advanced materials. In particular, the use of nitrile functional groups is appealing due to their intrinsic unidirectionality.[14–18] Herein, we detail the synthesis and X-ray characterization of 2-(dibromomethyl) benzonitrile (**1**, Fig. 1), which exhibits highly directional and unprecedentedly short C≡N···Br halogen bonds (HaBs) of 3.11 Å in the solid-state structure (Fig. 1). This is remarkable considering that compound **1** is not ionic and that the bromine atoms do not belong to a (hetero)aromatic system (C_{sp^2}-linked) but to an aliphatic one (C_{sp^3}-linked).[14,15] To elucidate the formation of these HaBs, in-depth density functional theory (DFT) calculations were employed. These calculations reveal that the antiparallel π-stacking arrangement of the aromatic rings amplifies both the electron-donating characteristics of the nitrile groups and the electron-accepting properties of the C–Br groups. Note that extremely short C≡N···Br halogen bonds (<3.2 Å) have been identified for purely (hetero)aromatic or π-conjugated systems (Fig. 1)[16] including those presenting metal ions or ionic species that significantly influence the natural electron density of the HaB system.[17,18] In the broad context, it is relevant to emphasize that ultrashort N···Br distances involving no nitrile groups, but more basic amines and pyridines are known.[19]

During the course of our studies in the development of supramolecular catalysis,[20] we synthesized and obtained

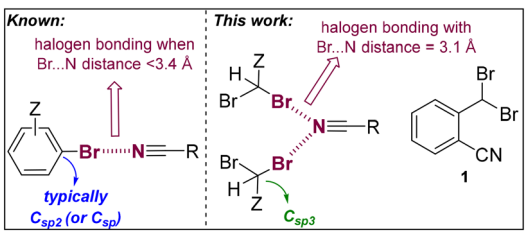

Fig. 1 Considerations of N···Br halogen bonding in aromatic systems (left) *versus* the current system (**1**, right) involving a non-aromatic bromide group. *Z* = any substitution pattern.

[a] *Univ. Rennes, CNRS, ISCR – UMR6226, F-35000 Rennes, France. E-mail: rafael.gramage-doria@univ-rennes1.fr*
[b] *Departament de Quimica, Universitat de les Illes Balears, Crta. de Valldemossa km 7.5, 07122 Palma de Mallorca, Baleares, Spain. E-mail: toni.frontera@uib.es*

† Electronic supplementary information (ESI) available: Synthesis and characterization of compounds, X-ray data and cartesian coordinates. CCDC 2330354. For ESI and crystallographic data in CIF or other electronic format see DOI: https://doi.org/10.1039/d4ce00307a

single crystals suitable for X-ray diffraction studies of **1** (Fig. 1). Most notably, the experimental C≡N···Br distance of 3.111 Å is significantly shorter than the sum of the van der Waals radii ($\sum R_{vdw}$ = 3.40 Å), and represents an unprecedented finding for a Br–C_{sp^3} σ-hole donor group.[14,15] The theoretical study herein, based on DFT calculations, analyzes the short (C≡N···Br–C_{sp^3}) halogen bonding interactions observed in the solid state of **1**. Initially, the unit cell of compound **1** was optimized using periodic boundary conditions, and the resultant geometry was then compared with the experimentally determined structure. As depicted in Fig. 2, both geometries exhibit nearly identical arrangements. The only difference lies in the position of the hydrogen atoms (the C–H bonds are marginally elongated in the DFT-optimized geometry). Intriguingly, the DFT calculations also reveal a significantly short (3.093 Å) halogen bond. Within the unit cell, beyond the formation of the halogen bond, an antiparallel π-stacking of compound **1** is evident, in good agreement between the experimental and theoretical π···π distances. The antiparallel π-stacking of compound **1** in the solid state is obvious from the X-ray molecular packing (Fig. S4 in the ESI†).

The unique short distance of the CN···Br halogen bond in **1** is somewhat surprising with respect to precedents in the literature,[14–18] especially considering that the sp-hybridized N atom of the nitrile group is not a strong Lewis base, and the σ-hole donor Br atom is not directly bonded to a potent electron-withdrawing group. We anticipated that the formation of π-stacked dimers might influence both the electron donor and acceptor groups. To investigate this hypothesis, we computed molecular electrostatic potential (MEP) surfaces for both the monomeric and dimeric forms of species **1**. As illustrated in Fig. 3, the σ-hole value at the Br atom notably increases by 70% from 14 kcal mol^{-1} in the monomer to 20.1 kcal mol^{-1} in the dimer. Additionally, the MEP value at the N atom of the nitrile group shifts from −33.8 kcal mol^{-1} in the monomer to −35.7 kcal mol^{-1} in the dimer. These observations clearly suggest a synergistic or cooperative effect between the π-stacking interaction and the halogen bonding. It is also noteworthy that in the monomer, the MEP maximum is located at the aromatic H atom *para* with respect to the nitrile substituent, marked at 27.6 kcal mol^{-1}, which decreases in the dimer down to 23.8 kcal mol^{-1}.

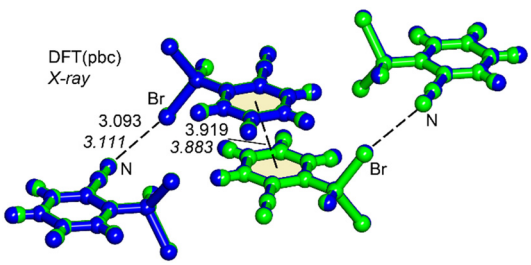

Fig. 2 Overlap of the X-ray (in green) and DFT (in blue) fully optimized unit cells of compound **1**. Distances in Å. The experimental distances are indicated in italics.

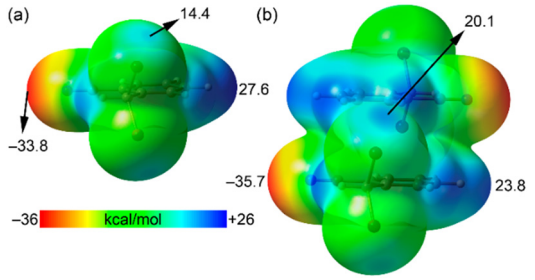

Fig. 3 MEP surfaces of 2-(dibromomethyl)benzonitrile (a) and its π-stacked dimer (b). The energies at selected points are given in kcal mol^{-1}. Isovalue 0.001 a.u.

Consequently, the difference between the MEP values at the maximum and the σ-hole is reduced in the dimer, indicating a complex interplay of interactions within the molecular structure.

Next, we conducted a thorough analysis of the halogen bonding, hydrogen bonding, and π-stacking interactions, both energetically and using a combination of quantum theory of atoms in molecules (QTAIM) and non-covalent interaction (NCI) plot analyses. The results are presented in Fig. 4(a). Initially, we examined the assembly observed in the unit cell, where the QTAIM analysis reveals a complex array of interactions. The π-stacking interaction is characterized by two bond critical points (BCPs) and bond paths connecting two carbon atoms of the aromatic ring. This interaction is further delineated by a green reduced density gradient (RDG)

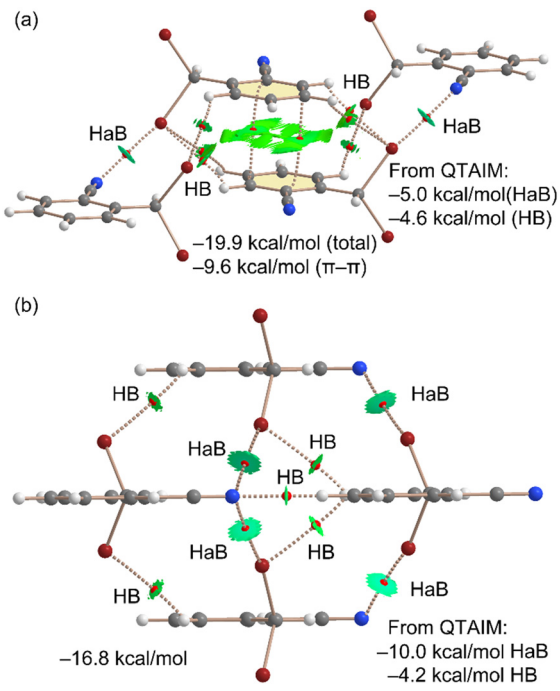

Fig. 4 QTAIM/NCIplot analyses of the unit cell (a) and HAB/HB (b) tetrameric assemblies of compound **1**. The formation energies and the contribution of the HaB and HBs derived from QTAIM are indicated (see computational methods in ESI†).

isosurface enveloping much of the region between the π-systems. Secondly, we identified two symmetrically equivalent halogen bonds, each marked by a BCP and a bond path linking the nitrogen atom to the bromine atom. These halogen bonds are additionally characterized by disk-shaped RDG isosurfaces, coinciding with the BCP locations. Furthermore, several CH···Br contacts also play a role in stabilizing the assembly, each indicated by a corresponding BCP, bond path, and green RDG isosurface. The total formation energy of this assembly is calculated to be −19.9 kcal mol^{-1}, with a significant contribution from the π-stacking interaction (−9.6 kcal mol^{-1}, calculated as a π-stacked dimer). The contributions from the halogen bonding and hydrogen bonding interactions were estimated using the QTAIM method, based on the potential energy density values at the BCPs (see theoretical methods in ESI† for details). Interestingly, the contribution of the two halogen bonds (−5.0 kcal mol^{-1}) is slightly more substantial than that of the hydrogen bonds (−4.6 kcal mol^{-1}). The involvement of bromine atoms in hydrogen bonds enhances the positive MEP value at the σ-hole, thereby explaining the more pronounced σ-holes in the dimer compared to the monomer.

Furthermore, a tetrameric assembly from **1** was analyzed using the QTAIM/NCIplot methodology, as shown in Fig. 4(b). In this tetramer, the absence of π-stacking leaves only halogen and hydrogen bonding available for consideration. As a result, a hydrogen bond is formed between the nitrile group and the hydrogen atom *para* with respect to the nitrile group of an adjacent molecule of **1**, aligning well with the MEP analysis, given the maximum and minimum MEP values of the interacting atoms. This nitrogen atom also forms two additional halogen bonds, resulting in a bifurcated halogen bond characterized by two CPs, bond paths, and green RDG isosurfaces. The contribution of the halogen bonds in this structure is −10.0 kcal mol^{-1} since a total of four HaBs are formed, and that of the hydrogen bonds is −4.6 kcal mol^{-1}, underscoring the significance of halogen bonds in the solid-state structure of compound **1**. The formation energy of this tetramer is −16.8 kcal mol^{-1}, slightly more negative than the summed QTAIM contributions of the halogen and hydrogen bonds (−14.2 kcal mol^{-1}). This discrepancy suggests either a minor underestimation by the QTAIM method or the presence of additional long-range van der Waals interactions among the monomers. The estimation of the hydrogen bond (HB) contribution utilizes the formula proposed by Espinosa *et al.*,[21a] expressed as $E = 0.5 \times V_b$, while the halogen bond contribution is calculated using the equation recommended by Bartashevich *et al.* ($E = 0.58 \times V_b$)[21b] where V_b represents the potential energy density at the bond CP.

To gain a deeper understanding of the interactions at play, an energy decomposition analysis (EDA) was performed on the halogen-bonded dimer depicted in Fig. 5. This analysis breaks down the total energy (E_{tot}) into its constituent parts: electrostatic (E_{el}), exchange-repulsion ($E_{ex\text{-}rep}$), orbital (E_{orb}), dispersion (E_{disp}), and correlation (E_{cor}). The findings, presented in Fig. 5, show that while all components

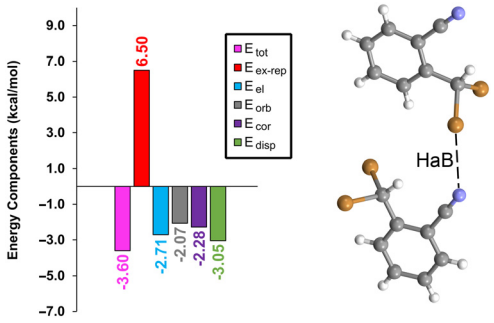

Fig. 5 EDA analysis of the dimer of **1** at the PBE0-D3/def2-TZVP level. Energies in kcal mol^{-1}.

contribute similarly, the dispersion effect stands out as slightly more significant (−3.05 kcal mol^{-1}, green bar) compared to the others, which range from −2.1 to −2.8 kcal mol^{-1}. Notably, the exchange-repulsion factor (indicated by the red bar) represents the most substantial contribution of 6.50 kcal mol^{-1}, yet it is effectively balanced by the attractive components. This detailed EDA sheds light on the complex and multifaceted nature of halogen bonding interaction in **1**.

Finally, we investigated whether orbital effects play a significant role in the bifurcated halogen bonds observed in the solid state of **1**. For this purpose, we utilized natural bond orbital (NBO) analysis, which is particularly effective for analyzing charge transfer effects. The donor–acceptor orbitals are depicted in Fig. 6, demonstrating a charge transfer from the lone pair (LP) orbital on the nitrogen atom to the antibonding σ*(Br–C) orbital, a characteristic feature of halogen bonding interactions. However, the stabilization energy associated with the LP(N) → σ*(Br–C) transfer is relatively modest, amounting to only 0.44 kcal mol^{-1}. This finding suggests that orbital effects are not the predominant factor driving the Br···N···Br interaction in this case.

In conclusion, the X-ray structure of 2-(dibromomethyl) benzonitrile (**1**) is reported herein, evidencing an intricate interplay of halogen bonding, hydrogen bonding, and π-stacking interactions in its solid-state structure. Through a

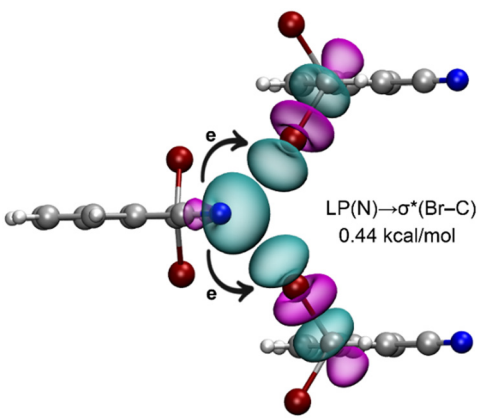

Fig. 6 NBOs involved in the bifurcated halogen bonds in a trimeric fragment of compound **1**. The $E^{(2)}$ energy is indicated.

combination of QTAIM, NCI plot, EDA, and NBO analyses, we demonstrated the significant role of these noncovalent interactions in stabilizing the molecular assembly. Our findings highlight the unexpectedly strong and short halogen bonds, taking into consideration the relatively weak Lewis base nature of the sp-hybridized N atom and the absence of strong electron-withdrawing groups directly bonded to the σ-hole donor Br atom. The π-stacking interaction has a crucial role in enhancing the strength of the HaBs electrostatically, as demonstrated using MEP surface analysis. This study provides valuable insights into the feasibility of C≡N···Br(C_{sp^3}-linked) halogen bonds that may find applications beyond crystal engineering.

Financial support from the CNRS and University of Rennes is acknowledged. A. F. thanks the MICIU/AEI from Spain for financial support (PID2020-115637GB-I00, FEDER funds). This project has received funding from the European Union's Horizon 2020 research program under the Marie Skłodowska-Curie grant agreement no. 899546 (K. K.).

Conflicts of interest

There are no conflicts to declare.

Notes and references

1 T. Clark, M. Hennemann, J. S. Murray and P. Politzer, in *Halogen Bonding I: Impact on Materials Chemistry and Life Sciences*, ed. P. Metrangolo and G. Resnati, Springer International Publishing, Cham, 2015, vol. 1, pp. 1–19.

2 (*a*) J. Bamberger, F. Ostler and O. G. Mancheño, *ChemCatChem*, 2019, **11**, 5198–5211; (*b*) C. Keuper, K. Fengler, F. Ostler, T. Danelzik, D. G. Piekarski and O. García Mancheño, *Angew. Chem., Int. Ed.*, 2023, **62**, e202304781.

3 W. Wang, Y. Wang, Y. Zhang, B. Ji, Y. Zhang and R. Wang, *Expert Opin. Drug Discovery*, 2019, **14**, 561–573.

4 (*a*) P. Metrangolo and G. Resnati, *Chem. – Eur. J.*, 2001, **7**, 2511–2519; (*b*) M. Malinska, I. Fokt, W. Priebe and K. Wozniak, *Cryst. Growth Des.*, 2015, **15**, 2632–2642.

5 P. Politzer, P. Lane, M. C. Concha, Y. G. Ma and J. S. Murray, *J. Mol. Model.*, 2007, **13**, 305–311.

6 J. S. Murray, Z. P. Shields and P. Politzer, *Int. J. Quantum Chem.*, 2010, **110**, 2823–2832.

7 D. M. P. Mingos, *Halogen Bonding, Fundamentals and Applications*, Springer-Verlag, Berlin, 2008.

8 P. Politzer, J. S. Murray and T. Clark, *Phys. Chem. Chem. Phys.*, 2010, **12**, 7748–7757.

9 E. Parisini, P. Metrangolo, T. Pilati, G. Resnati and G. Terraneo, *Chem. Soc. Rev.*, 2011, **40**, 2267–2278.

10 P. Metrangolo, F. Meyer, T. Pilati, G. Resnati and G. Terraneo, *Angew. Chem., Int. Ed.*, 2008, **47**, 6114–6127.

11 P. Metrangolo, H. Neukirch, T. Pilati and G. Resnati, *Acc. Chem. Res.*, 2005, **38**, 386–395.

12 L. C. Gilday, S. W. Robinson, T. A. Barendt, M. J. Langton, B. R. Mullaney and P. D. Beer, *Chem. Rev.*, 2015, **115**, 7118–7195.

13 (*a*) P. Metrangolo and G. Resnati, *Chem. – Eur. J.*, 2001, **7**, 2511–2519; (*b*) D. Yan, A. Delori, G. O. Lloyd, T. Friscic, G. M. Day, W. Jones, J. Lu, M. Wei, D. G. Evans and X. Duan, *Angew. Chem., Int. Ed.*, 2011, **50**, 12483–12486; (*c*) J. Wudarczyk, G. Papamokos, V. Margaritis, D. Schollmeyer, F. Hinkel, M. Baumgarten, G. Floudas and K. Mullen, *Angew. Chem., Int. Ed.*, 2016, **55**, 3220–3223; (*d*) S. Basurto, S. Garcia, A. G. Neo, T. Torroba, C. F. Marcos, D. Miguel, J. Barbera, M. B. Ros and M. R. de la Fuente, *Chem. – Eur. J.*, 2005, **11**, 5362–5376.

14 For C≡N···Br distances longer (3.12–3.19 Å) than the current report involving a non-aromatic system, see: (*a*) M. Shi and C.-J. Wang, *Tetrahedron*, 2002, **58**, 9063–9074; (*b*) A. Mori, H. Kawakami, N. Kato, S.-P. Wu and H. Takeshita, *Org. Biomol. Chem.*, 2003, **1**, 1730–1736; (*c*) K. Wright, B. Drouillat, L. Menguy, J. Marrot and F. Couty, *Eur. J. Org. Chem.*, 2017, 7195–7201; (*d*) C. J. Salomon, O. A. Mascaretti, C. E. Strouse and G. Punte, *Can. J. Chem.*, 1991, **69**, 578–583.

15 For a rare example with absence of discussion featuring a C≡N···Br distance of 3.0 Å in which the bromine atom is part of a highly electrophile (i.e. C_5Br_6), see: S. M. Rupf, P. Prohm and M. Malischewski, *Chem. Commun.*, 2020, **56**, 9834–9837.

16 For selected examples of short C≡N···Br distances involving (hetero)aromatic or π systems, see: (*a*) S. V. Baykov, S. I. Presnukhina, A. S. Novikov, A. A. Shetnev, V. P. Boyarskiy and V. Y. Kukushkin, *Cryst. Growth Des.*, 2021, **21**, 2526–2540; (*b*) A. D. Bond, J. Griffiths, J. M. Rawson and J. Hulliger, *Chem. Commun.*, 2001, 2488–2489; (*c*) A. S. Mikherdov, R. A. Popov, A. S. Smirnov, A. A. Eliseeva, A. S. Novikov, V. P. Boyarskiy, R. M. Gomila, A. Frontera, V. Y. Kukushkin and N. A. Bokach, *Cryst. Growth Des.*, 2022, **22**, 6079–6087; (*d*) L. Lai, B. Fang, M. Fan, W. Cheng and M. Yin, *J. Phys. Chem. C*, 2021, **125**, 16350–16357; (*e*) K. Liu, S. Li, L. Fu, Y. Lei, Q. Liao and H. Fu, *Nanoscale*, 2022, **14**, 6305–6311; (*f*) R. Mariaca, N.-R. Behrnd, P. Eggli, H. Stoeckli-Evans and J. Hulliger, *CrystEngComm*, 2006, **8**, 222–232; (*g*) X. Yuan, Y. Zhao, T. Zhan, J. Oh, J. Zhou, J. Li, X. Wang, Z. Wang, S. Pang, P. Cai, C. Yang, Z. He, Z. Xie, C. Duan, F. Huang and Y. Cao, *Energy Environ. Sci.*, 2021, **14**, 5530–5540; (*h*) P.-T. T. Pham and M. M. Bader, *Cryst. Growth Des.*, 2014, **14**, 916–922; (*i*) F. Frausto, Z. C. Smith, T. E. Haas and S. W. Thomas III, *Chem. Commun.*, 2015, **51**, 8825–8828; (*j*) Y. Imai, K. Kamon, S. Kido, T. Harada, N. Tajima, T. Sato, R. Kuroda and Y. Matsubara, *CrystEngComm*, 2009, **11**, 620–624; (*k*) A. D. Finke, S. Haberland, W. Bernd Schweizer, P. Chen and F. Diederich, *Angew. Chem., Int. Ed.*, 2013, **52**, 9827–9830; (*l*) H. Usta, C. Risko, Z. Wang, H. Huang, M. K. Deliomeroglu, A. Zhukhovitskiy, A. Facchetti and T. J. Marks, *J. Am. Chem. Soc.*, 2009, **131**, 5586–5608; (*m*) R. A. Wiscons, V. Coropceanu and A. J. Matzger, *Chem. Mater.*, 2019, **31**, 6598–6604; (*n*) T. Bjorvatten, *Acta Chem. Scand.*, 1968, **22**, 410–420.

17 For selected examples of short C≡N···Br distances involving metal-free ionic species, see: (*a*) J. Harloff, K. C. Laatz, S. Lerch, A. Schulz, P. Stoer, T. Strassner and A. Villinger, *Eur.*

J. Inorg. Chem., 2020, 2457–2464; (*b*) P. Arsenyan, J. Vasiljeva, S. Belyakov, E. Liepinsh and M. Petrova, *Eur. J. Org. Chem.*, 2015, 5842–5855; (*c*) S. V. Rosokha, C. L. Stern, A. Swartz and R. Stewart, *Phys. Chem. Chem. Phys.*, 2014, **16**, 12968–12979; (*d*) V. Figala, T. Gessner, R. Gompper, E. Hadicke and S. Lensky, *Tetrahedron Lett.*, 1993, **34**, 6375–6378.

18 For selected examples of short C≡N···Br distances involving the presence of metal ions, see: (*a*) S. Ohkoshi, S. Takano, K. Imoto, M. Yoshikiyo, A. Namai and H. Tokoro, *Nat. Photonics*, 2014, **8**, 65–71; (*b*) C. Rumo, A. Stein, J. Klehr, R. Tachibana, A. Prescimone, D. Haussinger and T. R. Ward, *J. Am. Chem. Soc.*, 2022, **144**, 11676–11684; (*c*) J. E. Ormond-Prout, P. Smart and L. Brammer, *Cryst. Growth Des.*, 2012, **12**, 205–216; (*d*) C. Ohde, T. Kusamoto, K. Nakabayashi, S.-I. Ohkoshi and H. Nishihara, *Cryst. Growth Des.*, 2017, **17**, 2203–2210; (*e*) S. Derossi, L. Brammer, C. A. Hunter and M. D. Ward, *Inorg. Chem.*, 2009, **48**, 1666–1677; (*f*) Y. Tsunobuchi, S. Kaneko, K. Nakabayashi and S. Ohkoshi, *Cryst. Growth Des.*, 2011, **11**, 5561–5566; (*g*) N. Jakupec, L. Fotovic and V. Stilinovic, *CrystEngComm*, 2020, **22**, 8142–8150; (*h*) B. Guo, X. Zhang, J.-H. Yu and J.-Q. Xu, *Dalton Trans.*, 2015, **44**, 11470–11481; (*i*) H. Petzold, P. Djomgoue, G. Horner, S. Heider, C. Lochenie, B. Weber, T. Ruffer and D. Schaarschmidt, *Dalton Trans.*, 2017, **46**, 6218–6229.

19 For selected examples of ultrashort N···Br distances involving no nitrile groups, see: (*a*) S. C. Blackstock and J. K. Kochi, *J. Am. Chem. Soc.*, 1987, **109**, 2484–2496; (*b*) J. A. Zerkowski, J. C. MacDonald and G. M. Whitesides, *Chem. Mater.*, 1994, **6**, 1250–1257; (*c*) R. Liantonio, P. Metrangolo, T. Pilati, G. Resnati and A. Stevenazzi, *Cryst. Growth Des.*, 2003, **3**, 799–803; (*d*) P.-H. Liu, L. Li, J. A. Webb, Y. Zhang and N. S. Goroff, *Org. Lett.*, 2004, **6**, 2081–2083; (*e*) L. Catalano, S. Perez-Estrada, H.-H. Wang, A. J.-L. Ayitou, S. I. Khan, G. Terraneo, P. Metrangolo, S. Brown and M. A. Garcia-Garibay, *J. Am. Chem. Soc.*, 2017, **139**, 843–848; (*f*) C. Weinberger, R. Hines, M. Zeller and S. V. Rosokha, *Chem. Commun.*, 2018, **54**, 8060–8063; (*g*) A. M. Abeysekera, B. B. Averkiev, P. Le Magueres and C. B. Aakeröy, *Org. Biomol. Chem.*, 2021, **19**, 6671–6681.

20 (*a*) P. Zardi, T. Roisnel and R. Gramage-Doria, *Chem. – Eur. J.*, 2019, **25**, 627–634; (*b*) N. Abuhafez and R. Gramage-Doria, *Faraday Discuss.*, 2023, **244**, 186–198.

21 (*a*) E. Espinosa, E. Molins and C. Lecomte, *Chem. Phys. Lett.*, 1998, **285**, 170–173; (*b*) E. V. Bartashevich and V. G. Tsirelson, *Russ. Chem. Rev.*, 2014, **83**, 1181–1203.